J Mater Sci (2010) 45:6505–6510
DOI 10.1007/s10853-010-4739-2

Characterization of $NaPO_3$–SnO–WO_3 glasses prepared by microwave heating

Sébastien Chenu · Ronan Lebullenger · Jean Rocherullé

Received: 31 March 2010 / Accepted: 25 June 2010 / Published online: 7 July 2010

Abstract Phosphate glasses containing tin and tungsten oxides were produced by microwave heating under a nitrogen protective atmosphere. Microwaves permit to heat the raw materials at temperatures close to 1000 °C in short time and to obtain homogeneous glasses in less than 10 min. All samples were characterized from thermal and mechanical point of view as function of metal oxide proportions. The equimolar addition of SnO and WO_3 in sodium phosphate matrix involves a linear evolution of the different properties (T_g, CTE, density, mechanical properties, and durability). Thus, we have shown a progressive strengthening of the network. The glass transition temperature does not exceed 405 °C, and the chemical durability is improved to four orders of magnitude. The dissolution rate is equal to 3.4×10^{-7} g cm^{-2} min^{-1} for $40NaPO_3$–$30SnO$–$30WO_3$ glass composition and is comparable with those of the window glass.

Introduction

Phosphate glasses generally have low melting temperature, large coefficient of thermal expansion, and a wide range of compositions is available. These glasses have been intensively studied for numerous applications: optical molding [1, 2], laser hosts [3], sealing glasses [4, 5], biomaterials [6], nuclear waste immobilization [7, 8], and solid electrolytes with high ionic conductivity [9, 10]. Nevertheless, the relative poor chemical durability often limits the use of phosphates glasses. However, it is possible to enhance the durability by different methods: the addition of refractory oxides like Al_2O_3, B_2O_3, Fe_2O_3 [11, 12], or the nitridation of glasses [13, 14] (i.e., the nitrogen for oxygen substitution in the vitreous network). The improvement of the chemical durability usually involves an increase of the glass transition temperature. An interesting challenge is to obtain the best compromise between a low glass transition temperature and a good chemical durability.

The addition of transition metal oxides in phosphate glasses could be an alternative route. Indeed, these elements could exist in several oxidation states in the glass matrix and influence the chemical durability. For example, Kumar et al. [15] have observed that the dissolution of CaO–P_2O_5–Fe_2O_3 glass is related to redox state of iron ions and it could vary from 25% as function of synthesis conditions.

Tungsten oxide is known to form glasses with $NaPO_3$ in a wide range of composition and to improve the chemical resistance against atmospheric moisture [16, 17] but with an increase of Tg. SnO and PbO can also be added to sodium metaphosphate ($NaPO_3$), and glass formation occurs over a wide range of compositions [18–20]. An interesting feature of these oxides is to reduce the glass transition temperature [5]. Tin oxide has been preferred to lead oxide because PbO is known to have deleterious health and environmental effects. The simultaneous addition of SnO and WO_3 to sodium metaphosphate could allow us to get glasses with low characteristic temperatures and good chemical durability.

In the present work, a domestic microwave oven was used to achieve the glass synthesis. The chemical composition of the glasses can be represented by the following formula:

S. Chenu · R. Lebullenger · J. Rocherullé (✉)
UMR CNRS 6226 Sciences Chimiques, Equipe Verres et Céramiques, Université de Rennes I, Campus de Beaulieu, 35042 Rennes, France
e-mail: Jean.rocherulle@univ-rennes1.fr
URL: http://www.verceram.univ-rennes1.fr/

$(100 - 2x)NaPO_3 - xSnO - xWO_3$,

x varying from 0 to 30. Using different experimental techniques, we report several thermal and physical characteristics such as glass transition temperature (T_g), coefficient of thermal expansion (CTE), density, the different elastic moduli and viscosity. The chemical durability of these glasses has been measured at 50 °C on bulk samples in water.

Experimental

Glasses have been elaborated by a simple microwave melting method [21–24]. The microwave route offers several advantages over conventional methods, the foremost of which are the very short time scales required for the preparation and the homogeneity of the heating. Indeed, heat is generated within the sample by interaction between molecules and the magnetic field, while in a resistive furnace energy is transmitted to the surface of the sample and then to the all volume by conduction [25]. A critical requirement is the coupling of at least one of the reactants to the microwave field to initiate and drive the heating. In a typical experiment, required quantities of starting materials, $NaPO_3$ (Aldrich), SnO (99.9% Alfa Aesar), WO_3 (99+% Aldrich) are placed in a clean silica crucible and exposed to microwave irradiation up to 10 min in a domestic microwave oven (Kerwave®, 2.45 GHz, 750 W nominal power) under a nitrogen flow (150 L h^{-1}). The crucible is covered by a cap in silica that allows the simultaneous transfer of nitrogen and exhaust gas from the melt. This provides a protective atmosphere avoiding oxidation of tin. After 10 min, the melt is poured between two stainless steel plates and the glass is annealed for 1 h at T_g to relieve residual stress before cooling down slowly to room temperature. During the glass synthesis, an optical pyrometer (IGA 140 Impac®) is used to monitor the temperature of the melt.

The amorphous nature of the sample was checked by X-ray powder diffraction (XRD). Data were collected at room temperature with a PHILIPS diffractometer (Model PW 1830) using CuK_α radiation ($K_{\alpha1} = 1.5406$ Å, $K_{\alpha2} = 1.5444$ Å) selected with a diffracted-beam graphite monochromator and the Bragg–Brentano optics. The 10–70° (2θ) angular range was scanned in 0.02° (2θ) steps with a counting time set at 1 s $step^{-1}$. The ICDD PDF database, available in the program search/match from the PC software package X'PERT supplied by PHILIPS, was interrogated to reveal possible crystallization.

The viscosity–temperature curve of the glasses has been determined by the parallel plate method, for viscosities in the range 10^9–10^4 Poise. The measurements were performed with a Theta Industries® parallel plate viscometer with a heating rate of 5 °C min^{-1} and a load of 200 g. The viscosity–temperature curve, above T_g, has been extrapolated from experimental data using the Vogel–Fulcher–Tamman (VFT) model. According to this model, the viscosity–temperature relation can be expressed as:

$$\log \eta = A + \frac{B}{T - T_o}, \quad (1)$$

where A, B, and T_o are constants.

The glass transition temperature was determined from DTA experiments conducted at 10 °C min^{-1} and performed with a TA instruments® SDT 2960. The overall accuracy of this instrument is expected to be within ±2 °C. The coefficient of thermal expansion (CTE) was calculated from a thermomechanical experiment (TA Instruments® Model TMA 2940) performed with a 5 °C min^{-1} heating rate and a preload force of 0.1 N. The precision of the CTE determination is $\pm 2 \times 10^{-7}$ K^{-1} in the 50–250 °C range.

The density of the samples was measured at room temperature using Archimedes method with absolute alcohol as immersion fluid. The error in the determination of the density is ±0.02 g cm^{-3}.

Young's modulus (E), bulk modulus (G), and shear modulus (K) were calculated from experiments using the ultrasonic velocity technique. This technique is based on time-of-flight measurements using the pulse-echo technique [26]. Vickers microhardness measurements have been carried out on Matsuzama® MXT 70 equipment by the indentation technique using a 50-g load applied for 5 s.

The chemical durability was evaluated from the weight loss of bulk samples immersed in water at 50 °C using static method [27]. A constant ratio sample surface/solution volume of 0.1 cm^{-1} was maintained to compare the results. The faces of the samples were polished with 1200 grit SiC paper and cleaned in alcohol. After each corrosion test, the samples were dried at 100 °C until the weight remained constant. The dissolution rate (DR) of samples has been calculated from the measured weight loss (ΔW), sample surface area (SA), and time of immersion (t), using the following equation:

$$DR = \frac{\Delta W\ (g)}{SA\ (cm^2)\ \times\ t\ (min)}. \quad (2)$$

The error in the average reported herein is estimated at 5%. During these durability tests, the pH is measured with a Schott® CG819 pH-meter and the precision is ±0.05.

Results and discussion

Glass synthesis

Figure 1 shows the heating temperature profiles obtained for sodium phosphate glasses with various tin and tungsten

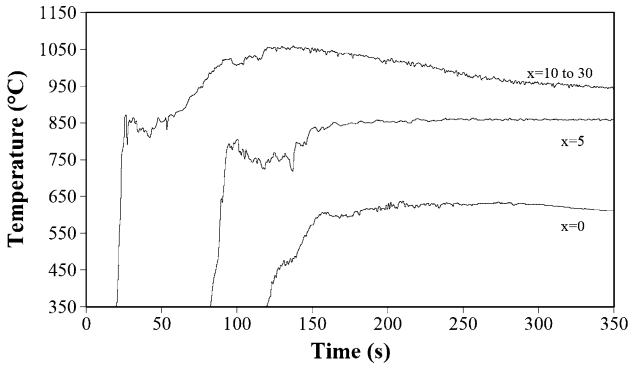

Fig. 1 Melting temperature profile of $(100 - 2x)NaPO_3$–$xSnO$–xWO_3 glasses

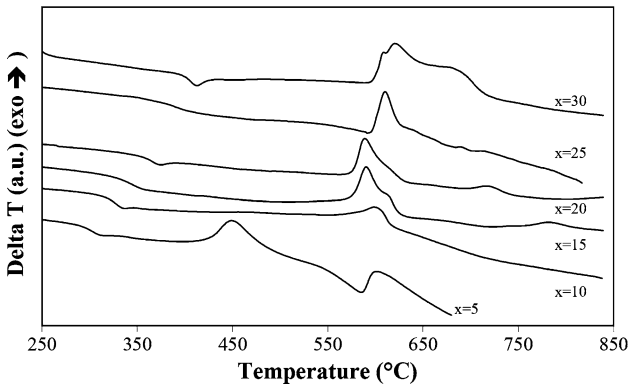

Fig. 2 DTA curves of $(100 - 2x)NaPO_3$–$xSnO$–xWO_3 glasses under air

oxide contents. The weight of the batch, the crucible, and its position inside the microwave oven are reminded the same.

The addition, in equimolar proportion, of SnO and WO_3 to sodium metaphosphate causes an increase of the batch temperature and a decrease of the starting reaction time. If one compares the temperature profiles of the tin and tungsten samples for which x is 10 to the pure metaphosphate, the melting temperature increases by 300 °C. In addition, the decrease in induction time for heating is about 100 s. However, we have not found any additional variations for samples containing higher quantities of transition metal oxides. In all cases, the melting temperature reaches a plateau close to 950 °C. In a previous paper concerning $SnO–P_2O_5$ binary glasses [28], we have observed the same behavior for the temperature profiles.

The heating of the mixture depends on the response of the material to the microwave exposure, in other terms the dielectric constant and the dielectric losses. The addition of metal oxides, such as SnO and WO_3, to $NaPO_3$ increases the temperature of the melt and decreases the induction time for heating because SnO and WO_3 are better microwave absorbers than sodium metaphosphate. Nevertheless, the dielectric constant and dielectric loss of the mixture are temperature-dependent quantities, thus we can assume that a limit of heat dissipation is achieved leading to a maximum temperature independent of the chemical composition.

Devitrification behavior

All as-prepared materials show a broad diffraction halo in the X-ray diffraction patterns (not presented here) which are typical for amorphous structures and attest the absence of crystalline phase formation during the synthesis.

Each powdered glass has been analyzed up to 850 °C by DTA experiments as illustrated in Fig. 2. Only the composition for which $x = 5\%$ presents an endothermic peak corresponding to the melting of a crystalline phase. Indeed,

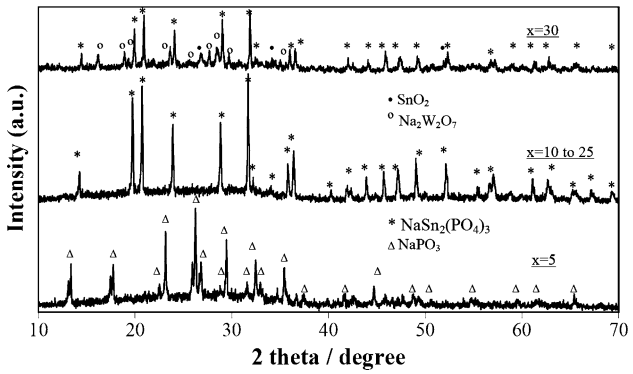

Fig. 3 XRD patterns obtained for studied samples after treatment at 850 °C

each sample presents an endothermic phenomenon corresponding to the glass transition followed by an exothermic peak due to the crystallization of one or several phases.

Figure 3 depicts the X-ray diffraction patterns of each sample after DTA treatment until 850 °C. For $x = 5\%$, the crystalline phase is identified to $NaPO_3$ (ICCD11-0648). For samples characterized by x values in the range from 10 to 25%, there is also a unique phase identified to $NaSn_2(PO_4)_3$ (ICCD 49-1198) with a NZP type structure. For $x = 30\%$, there are three phases which are, respectively, identified to $NaSn_2(PO_4)_3$ (ICCD 49-1198), SnO_2 (ICCD 03-0439), and $Na_2W_2O_7$ (ICCD 31-1185).

The glass with $x = 5\%$ presents an endothermic peak at 570 °C due to the melting of crystallized $NaPO_3$, while the other compositions do not show any endothermic phenomenon until 850 °C. Indeed, when x is greater than 5%, a crystalline phase, identified to $NaSn_2(PO_4)_3$, appears around 600 °C and attests to the modification of oxidation state of tin. As mentioned in [29], there is a direct oxidation of Sn^{2+} by atmospheric oxygen, and the formation of Sn^{4+} ions is accompanied by crystallization of $NaSn_2(PO_4)_3$. This phase is known to be stable in temperature [30] explaining the absence of exothermic peaks in the case of

compositions for which $x > 5\%$. Moreover, the presence of SnO_2 when $x = 30\%$ gives raise to the oxidation of tin (II) oxide. The broadening of crystallization peak for this sample is probably a consequence of the occurring of the $Na_2W_2O_7$ phase.

Physical characteristics

The evolution of different physical properties of glasses is shown in Fig. 4. For an increase of the metal oxides content from 5 to 30%, the glass transition increases linearly from 303 to 405 °C. The density and the different elastic moduli present a similar linear variation. On the contrary, there is a linear decrease of the thermal expansion coefficient.

The introduction of metal oxides in a sodium metaphosphate glass causes a strengthening of the vitreous network, leading to a simultaneous increase of the T_g and elastic moduli and to a decrease of the CTE. Thus, it has been shown in [16] and [31] that a sodium metaphosphate glass containing 20 mol.% of WO_3 has a T_g of 382 °C and a Young's modulus of 51 GPa, values which can be compared to those of the $NaPO_3$ glass, 260 °C and 35 GPa, respectively. The effect of the SnO addition to the same parent glass leads to a smaller increase of these quantities, 323 °C and 40 GPa, respectively [29, 32]. According to [19], SnO plays a dual structural role, first as a modifier up to 33 mol.% and then as a network former above 33 mol.%. The simultaneous addition of 10 mol.% of SnO and 10 mol.% of WO_3 leads to an intermediate behavior where the T_g remains almost stable (327 °C) while the Young's modulus increases (46 GPa).

In first approximation, density can be considered as an additive property. The density increases monotonously with the addition of SnO and WO_3 because $NaPO_3$ has a lower density than SnO and WO_3 (respectively, 2.49, 6.45, and 7.20 g cm^{-3}). In the same way, we calculated the molar volume of each studied glasses, however, these values increase monotonously with the $NaPO_3$ content. This parameter does not allow us to highlight any structural change.

Figure 5 represents the viscosity of the different studied glasses as a function of temperature. As mentioned in the experimental section, the viscosity values have been calculated with a relatively good fit to viscosity data over a wide viscosity range, the constants of the VFT equation being given in Table 1. At a constant temperature, the viscosity can grow from several orders of magnitude when the metal oxides content is increasing. This is consistent with the strengthening of the vitreous network induced by the presence of metal oxides. The compositional dependence of the viscosity of glass forming melts is closely related to the connectivity of the structure. Thus, changes in composition which enhance connectivity increase the

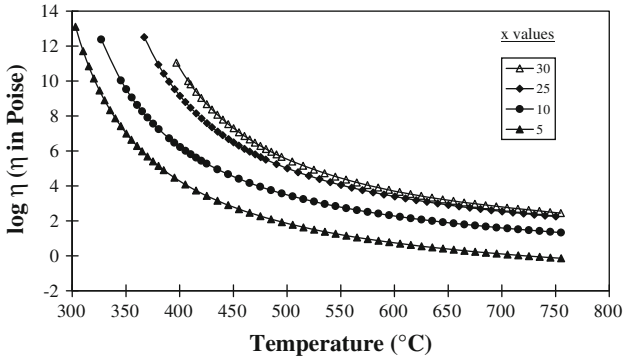

Fig. 5 Viscosity–temperature curves for several studied glasses

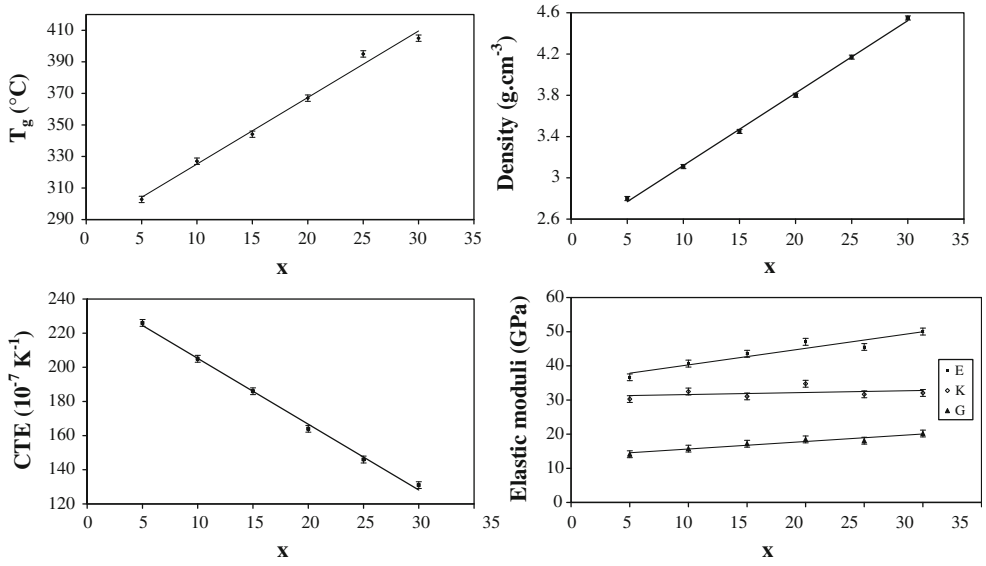

Fig. 4 Physical and chemical characteristics of $(100 - 2x)NaPO_3$–$xSnO$–xWO_3 glasses

Table 1 Constants of the VFT equation for $(100 - 2x)NaPO_3$–$xSnO$–xWO_3 glasses

x	5	10	25	30
A	−2.24	−0.84	−0.24	−0.05
B	1100	1115	1187	1154
T_o (K)	504	516	547	566

viscosity. W is a transition metal capable of existing in multiple valence states such as +5 or +6. These entities are present in octahedral coordination, distorted in the case of W^{5+}. In the presence of a modifier like Na_2O, we can expect that a modification occurs first at the W–O–W linkage due to the clear hierarchy of bond energies (i.e., $E_{P-O-P} > E_{W-O-P} > E_{W-O-W}$). It causes a structural rearrangement in the phosphorus tetrahedra modifying the connectivity of the network [33].

The chemical durability is measured by the weight loss method in water at 50 °C. Figure 6 shows pH evolution as function of immersion time. We observe a fast decrease in pH in the first minutes of experiment and a stabilization around pH 5 for longer immersion times. We can note that the decrease in pH is more important for glasses with $x \leq 20$ mol.% ($\Delta \sim 1.9$ pH unit) than for the other compositions ($\Delta \sim 0.8$ pH unit). Whatever the composition, the pH stabilization is observed.

Figure 7 represents the glass dissolution rates as function of time. The dissolution velocity is very high (10^{-2} g min^{-1} cm^{-2}) in the first minutes of experiments. Then, it strongly decreases (10^{-4} to 10^{-7} g min^{-1} cm^{-2}) and stabilizes after 3 h. Table 2 summarizes the logarithm of the average dissolution rates and the corresponding values of the T_g. As one can see, it varies from −2.51 to −6.47 g min^{-1} cm^{-2} with the metal oxides content increase. Furthermore, the chemical durability is clearly correlated to the T_g value. The decrease of pH in the first minutes of experiment is due to the formation of tungstic acid because the dissolution of pure tin phosphate glass does not present variation of pH while there is an important

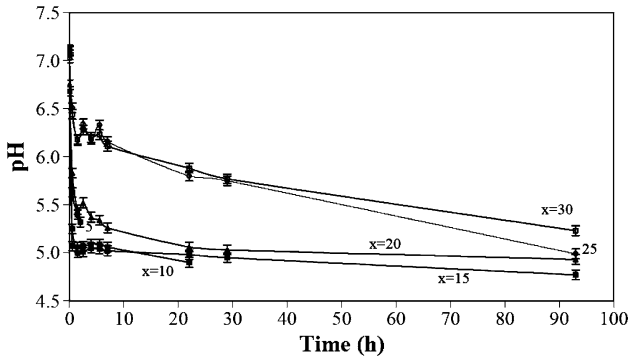

Fig. 6 pH evolution of durability solutions as function of time

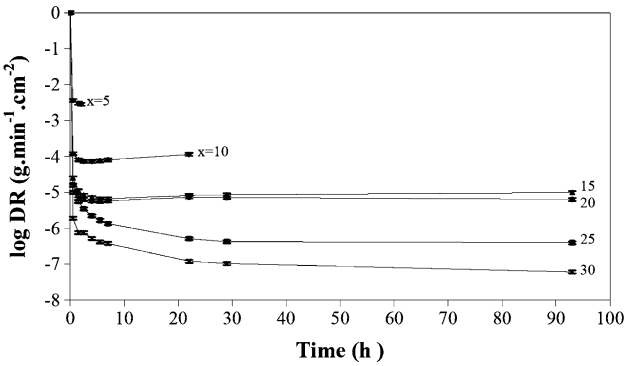

Fig. 7 Chemical durability of $(100 - 2x)NaPO_3$–$xSnO$–xWO_3 glasses as function of time

Table 2 Chemical durability and glass transition temperature of $(100 - 2x)NaPO_3$–$xSnO$–xWO_3 glasses

x	5	10	15	20	25	30
log DR (g min^{-1} cm^{-2})	−2.51	−4.07	−5.04	−5.17	−5.77	−6.47
T_g (°C)	303	327	344	367	395	405

pH decrease for phosphate glass containing tungsten oxide. After this decrease, the stabilization of pH around 5 is probably due to the saturation of solution because the tests are realized in static method. The time to obtain this saturation is even more important that the dissolution rate is low. The curves obtained for dissolution velocity and pH present a similar evolution. The chemical durability of glass is improved 10,000 times when x increases from 5 to 30%, while the values of T_g only increase from 100 °C. The best dissolution rate is equal to 3.4×10^{-7} g cm^{-2} min^{-1}. This value is very low for a phosphate glass, and the chemical durability of this composition can be considered as acceptable. For comparison, a borosilicate glass immersed in the same conditions has a chemical durability close to 10^{-8} g cm^{-2} min^{-1} [8].

Conclusion

The present study has demonstrated the feasibility to produce phosphate glasses in the ternary system $NaPO_3$–SnO–WO_3 by using a domestic microwave oven. In this way, homogeneous samples can be obtained within short times. The equimolar addition of SnO and WO_3 until 30% causes a linear variation of several physical properties due to the strengthening of the vitreous network. Moreover, the chemical durability of the glass with $x = 30$ is comparable with those of a window glass. This improvement is accompanied by a moderate increase of T_g, giving an appreciable compromise between durability and low

characteristic temperature. Thus, we can expect potential applications like waste immobilization for these materials. Another interest is the possibility to obtain after heat treatment, glass–ceramics with a single NZP phase. This type structure is usually known for generating high alkali ionic conductivity. Thus, we can envisage the use of these glass–ceramics as solid electrolytes.

References

1. Takebe H, Nonaka W, Kubo T, Cha J, Kuwabara M (2007) J Phys Chem Solids 68:983
2. Wen L, Jijian C (2001) Glass Technol 42:153
3. Campbell JH, Suratwala TI (2000) J Non-Cryst Solids 263–264:318
4. Donald IW (1993) J Mater Sci 28:2841. doi:10.1007/BF01117591
5. Morena R (2000) J Non-Cryst Solids 263–264:382
6. Abou Neel EA, Pickup DM, Valappil SP, Newport RJ, Knowles JC (2009) J Mater Chem 19:690
7. Day DE, Ray CS, Marasinghe GK, Karabulut M, Fang X (2000) Final report (doi:10.2172/827407) 1
8. El Hadrami A, Aouad H, Mesnaoui M, Maazaz A, Videau JJ (2002) Mater Lett 57:894
9. Martin SW (1991) J Am Ceram Soc 74:1767
10. Muñoz F, Durán A, Pascual L, Montagne L, Revel B, Rodrigues ACM (2008) Solid State Ionics 179:574
11. Donald IW, Metcalfe BL, Fong SK, Gerrard LA (2006) J Non-Cryst Solids 352:2993
12. Brow RK (1993) J Am Ceram Soc 76:913
13. Le Sauze A, Montagne L, Palavit G, Marchand R (2001) J Non-Cryst Solids 293–295:81
14. Day DE (1989) J Non-Cryst Solids 112:7
15. Kumar B, Lin S (1991) J Am Ceram Soc 74:226
16. de Araujo CC, Strojek W, Zhang L, Eckert H, Poirier G, Ribeiro SJL, Messaddeq Y (2006) J Mater Chem 16:3277
17. Poirier G, Ottoboni FS, Cassanjes FC, Remonte A, Messaddeq Y, Ribeiro SJL (2008) J Phys Chem B
18. Vaidhyanathan B, Prem Kumar C, Rao JL, Rao KJ (1998) J Phys Chem Solids 59:121
19. Harish Bhat M, Berry FJ, Jiang JZ, Rao KJ (2001) J Non-Cryst Solids 291:93
20. Bekaert E, Montagne L, Delevoye L, Palavit G, Wattiaux A (2004) J Non-Cryst Solids 345–346:70
21. Vaidhyanathan B, Ganguli M, Rao KJ (1994) J Solid State Chem 113:448
22. Rao KJ, Vaidhyanathan B, Ganguli M, Ramakrishnan PA (1999) Chem Mater 11:882
23. Ghussn L, Martinelli JR (2004) J Mater Sci 39:1371. doi:10.1023/B:JMSC.0000013899.75724.e1
24. Duval DJ, Phillips BL, Terjak MJE, Risbud SH (1997) J Solid State Chem 131:173
25. Thostenson ET, Chou TW (1999) Composites A 30:1055
26. Blessing GV (1990) ASTM STP 1045, Philadelphia, PA, USA, p 1045
27. Takebe H, Baba Y, Kuwabara M (2006) J Non-Cryst Solids 352:3088
28. Hémono N, Chenu S, Lebullenger R, Rocherullé J, Kéryvin V, Wattiaux A (2010) J Mater Sci 45:2916. doi:10.1007/s10853-010-4283-0
29. Chenu S, Rocherullé J, Lebullenger R, Merdrignac O, Cheviré F, Tessier F, Oudadesse H (2010) J Non-Cryst Solids 356:87
30. Breval E, Harshe G, Agrawal DK (1995) J Mater Sci Lett 14:728
31. Muthupari S, Lakshmi Raghavan S, Rao KJ (1996) Mater Sci Eng B 38:237
32. Bhat H, Ganguli M, Rao KJ (2003) Bull Mater Sci 26:407
33. Selvaraj U, Rao KJ (1985) J Non-Cryst Solids 72:315